Available online at www.sciencedirect.com
ScienceDirect
Trans. Nonferrous Met. Soc. China 20(2010) 577−583
Transactions of Nonferrous Metals Society of China
www.tnmsc.cn

Microstructure of in situ Al_3Ti/6351Al composites fabricated with electromagnetic stirring and fluxes

LI Gui-rong(李桂荣), WANG Hong-ming(王宏明), ZHAO Yu-tao(赵玉涛),
CHEN Deng-bin(陈登斌), CHEN Gang(陈 刚), CHENG Xiao-nong(程晓农)

Institute of Materials Science and Engineering, Jiangsu University, Zhenjiang 212013, China

Received 27 February 2009; accepted 25 August 2009

Abstract: The 6351 wrought aluminum alloy and K_2TiF_6-CaF_2-LiCl components were selected as raw materials to fabricate in situ Al_3Ti particulate reinforced aluminum alloy at 720 ℃ via direct melt reaction method with electromagnetic stirring (EMS). CaF_2 and LiCl acted as fluxes to lower the reaction temperature of the system. It is shown that the electromagnetic stirring and fluxes accelerate the emulsion process of K_2TiF_6. Optical microscopy, scanning electron microscopy, transmission electron microscopy and energy dispersive spectrum were utilized to analyze the microstructure and components of composites. Compared to composites fabricated without EMS and fluxes, the sizes of endogenetic Al_3Ti are refined from 10−15 μm to 2−4 μm, which are often accompanied with silicon element. The morphology of Al_3Ti or $Al_3TiSi_{0.22}$ exhibits triangle, quadrilateral and other clumpy patterns. Because of the Ca elements from CaF_2, the sizes of Mg_2Si decrease from 8−10 μm to 1−2 μm due to the formation of Ca_2Si.

Key words: 6351 Al alloy; microstructure; in situ particle reinforced aluminum composites; electromagnetic stirring; fluxes

1 Introduction

In recent years, the demands for new materials with excellent comprehensive properties become stronger and stronger[1−3]. The necessary characteristics of advanced functional and structural materials include high specific modulus, strength, hardness, ductility, corrosion resistance, low heat expansion coefficient, abradability and so on[4−5]. Over the past twenty years, considerable attentions have been paid to the particles reinforced metal matrix composites (abbreviated PRMMCs), especially the aluminum matrix ones which were developed rapidly due to their good performances and competitive cost[6−7]. The aerospace, automotive industries and other structural applications promote their developments, too.

Among all the reinforced particles, transition-metal trialuminide intermetallics such as Al_3Zr and Al_3Ti are good candidates for the in situ reinforcements of light metal matrix[8−9], which have low densities and high elastic modulus. YIN et al[10] selected Al-TiO_2 to fabricate Al_3Ti/Al at the reaction temperature of 1 000−1 200 ℃. Later, more attentions were paid to K_2TiF_6 as the source of Ti element in Al_3Ti. Not only its low cost but also the lower reaction temperature than that of Al-TiO_2 system attributes to the decrease of the sizes of Al_3Ti particles. 6351 wrought aluminum has been utilized in the architecture, automobile, pipes and so on due to its middle strength and high elongation (T6 condition, tensile strength σ_b=310 MPa, yield strength σ_s=283 MPa, δ=14.2%)[11]. However, the strength is not strong enough to act as some important structures. It is necessary to explore new ways to fabricate new materials using the wrought alloy as matrix.

In this work, 6351 wrought aluminum alloy is selected as matrix and K_2TiF_6 salt is utilized to fabricate in situ Al_3Ti reinforced 6351 aluminum wrought alloy composites with electromagnetic stirring. The main aim is to lower the temperature of reaction system and the particle size of Al_3Ti. The thermodynamic process and microstructure of Al_3Ti/6351 composites are studied in

Foundation item: Project(2007AA03Z548) supported by the National High-Tech Research and Development Program of China; Project(207038) supported by the Key Program of Ministry of Education of China; Project(06-D-021) supported by the Talents Peak in Six Key Fields of Jiangsu Province in China; Project(07JDG084) supported by the Technical Enablement Foundation for the Super Special Talents of Jiangsu University; Project(20071108) supported by the Technical Enablement Foundation of Ministry of Education for the Returned Scholars; Project(20060299006) supported by the PhD Programs Foundation of Ministry of Education of China

Corresponding authors: ZHAO Yu-tao; Tel: +86-511-88797658; E-mail: zhaoyt@ujs.edu.cn; LI Gui-rong; Tel: +86-13951408072; E-mail: whmlgr@ujs.edu.cn

DOI: 10.1016/S1003-6326(09)60181-3

detail.

2 Experimental

2.1 Materials and sample preparation

The compositions of 6351 wrought aluminum alloy were (mass fraction): 0.7%−1.3% Si, 0.4%−0.8% Mg, 0.4%−0.8% Mn, <0.5% Fe, <0.2% Zn, <0.2% Ti, <0.1% Cu.

In order to reduce the initial melt temperature, CaF_2 and LiCl were added as fluxes. The mass ratio of mixture K_2TiF_6, CaF_2, LiCl is 80:15:5. The melting points of pure K_2TiF_6, CaF_2 and LiCl are 682, 1418 and 605 ℃, separately. The mass ratios of mixture were optimized via testing melting points through semi sphere method. The melting point of batched mixture was 486 ℃, which was decreased by 29% compared to that of pure K_2TiF_6.

Firstly, the K_2TiF_6 salt (industry reagents, >99.5%) was pre-heated to dehydrate the bounded water in electric oven at 250 ℃ for 3 h. Then, it was cooled, ground and screened together with CaF_2 and LiCl. At the same time, the Al alloy ingot was melted in an electric furnace under an argon atmosphere and held at 720 ℃ (while without using fluxes the furnace temperature should be controlled at 800℃). Certain amount of dehydrated reactants powder covered by aluminum foils was added into the melt with graphite bell, so the in situ reaction between the aluminum alloy melt and added salts took place instantly. An electromagnetic stirrer (DJMR-1616W) was utilized to increase the mass transfer during the whole in situ reaction. The electric furnace was placed at the cavity center of stirrer, where the average magnetic induced intensity of electromagnetic stirring apparatus was 0.025 T. The reaction time was controlled as 3 min, then the subsidiary products of in situ reaction were removed and the composite melt was refined by CCl_6 and stewed for several minutes. The composite melt was cast by semi continuous casting at 710−720 ℃ and cooled at 40−60 ℃/s. The diameter of the billet was 100 mm.

2.2 Characterization

The sample was ground, polished and tectorial membraned so as to observe the microstructure clearly. LEICA DM 2500M optical microscope (OM), JSM-7001F scanning electronic microscope (SEM), Inca Energy 350 energy dispersive spectrum (EDS), JEOL-JEM-2100-HR transmission electronic microscope (TEM) and D/max-2500PC X-ray diffractometer (XRD) were used to observe the microstructure and analyze the phases in composites. STA449C DSC (differential scanning calorimetry) was utilized to analyze the thermal effect of the chemical reaction between Al powder and K_2TiF_6, at a heating rate of 5 ℃/min without protective atmosphere.

The theoretical volume fraction of Al_3Ti particles was set as 3% (volume fraction). The recovery rate of K_2TiF_4 was presumed as 90%. The mass fraction of added K_2TiF_6 to the matrix is 7.68%. The elementary components in composites were nominated as: 1.1%Si-0.67%Mg-0.4%Mn-1.2%Ti-0.7%Ca-0.2%Cu-0.02%Cr-0.01%Fe-Al (Bal.). The mass ratio of Mg to Si was 0.61. It was less than 1.73, which was the mass ratio of Mg to Si in Mg_2Si particle. The mass fraction and volume fraction of Mg_2Si reinforced particles in the matrix were 1.11% and 1.69%, respectively.

3 Results and discussion

3.1 Thermodynamics and kinetics of in situ reaction

The integral chemical reaction between K_2TiF_6 and molten Al is deduced as

$$13Al+3K_2TiF_6=3Al_3Ti+K_3AlF_6+3KAlF_4 \quad (1)$$

According to the second law of thermodynamics, the Gibbs free energy ΔG of the reaction system can be expressed as:

$$\Delta G=\Delta H-T\Delta S \quad (2)$$

where H, S and T stand for the enthalpy, entropy and thermodynamic temperature respectively. At certain temperature, the ΔG_T can be expressed as:

$$\Delta G_T=\sum V_i\Delta G^\Theta+\int_{298}^{T}(\sum V_r c_{p,r}\mathrm{d}T)-\int_{298}^{T}(\sum V_P c_{p,P}\mathrm{d}T) \quad (3)$$

where G^Θ is the standard Gibbs free energy, $c_{p,r}$ and $c_{p,P}$ are the specific heat capacity at constant pressure of reactants and products, respectively; V_r and V_P are the mole volume fraction of reactants and products, respectively. Some thermodynamic parameters of involved substances in Eq.(1) are listed in Table 1.

Accordingly, the ΔG_T of in situ reaction of Al-

Table 1 Some thermodynamic parameters of reactants and products in Eq.(1)

Phase	ΔH^Θ/ (kJ·mol^{-1})	ΔG^Θ/ (kJ·mol^{-1})	$c_{p,r}$ or $c_{p,P}$/ (kJ·mol^{-1}·K^{-1})
Al	10.4	−323.8	$2.13+4.43\times10^{-3}T-4.91\times10^5T^{-2}$
K_2TiF_6	−665.4	−684.4	$51.45+15.56\times0^{-3}T-4.22\times10^5T^{-2}$
Al_3Ti	−142.3	−46.1	$103.51+6.76\times0^{-3}T-8.67\times10^5T^{-2}$
K_3AlF_6	−795.0	−815.3	$56.98+16.00\times0^{-3}T-7.92\times0^5T^{-2}$
$KAlF_4$	−275.2	−462.3	$33.57+14.12\times10^{-3}T$

K_2TiF_6 components can be calculated as

$$\Delta G_T = -15\ 489.45 + 12.87T + 0.13\times10^{-3}T^2 - 1.94\times10^5\ T^{-1} \quad (4)$$

When the system temperature is 993 K (720 ℃), the corresponding ΔG_T is −186 kJ/mol, so the in situ chemical reaction between Al and K_2TiF_6 salt will take place spontaneously.

Fig.1 shows the DSC curve of the thermo process of Al-10%K_2TiF_6 (mass fraction). At 452.4 ℃ and 606.3 ℃, there exists an apparent exothermal peak respectively. While from 796.3 ℃ the slope coefficient is larger than the heating-up velocity, which demonstrates that there is an exothermal reaction. Connecting the ΔG^Θ values the three exothermal reactions are deduced as

$$2Al+3K_2TiF_6 = 2K_3AlF_6+6[F]+3[Ti] \text{ (at 452.4 ℃)} \quad (5)$$

$$2Al+K_2TiF_6+2[F] = 2KAlF_4+[Ti] \text{ (at 606.3℃)} \quad (6)$$

$$3Al+[Ti] = Al_3Ti \quad (7)$$

Among the products, intermetallic compound Al_3Ti is the reinforced particle. Some properties of Al_3Ti and other pure substances in the composites are listed in Table 2.

Al_3Ti in the as-cast composites comes from two ways. One is the resultant of chemical reaction as Eq.(1), the other is the precipitate of molten Ti and Al atoms during solidification. The process can be illustrated in Fig.2.

When the volume fraction of Al_3Ti in melt is 3%, the mole ratio of Ti element to Al element is about 2:98.

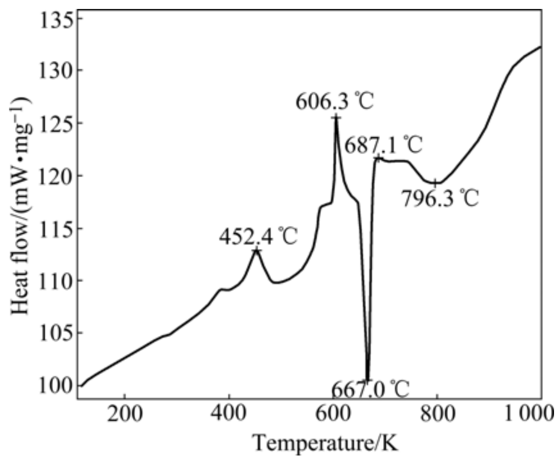

Fig.1 DSC curve of Al-10%K_2TiF_6

The component is shown as point A in Fig.2(a). The corresponding liquidus temperature is about 900 ℃. In the in situ process, the melt is stable at 720 ℃ (point B) when the solid Al_3Ti precipitates. If the system is at equilibrium state, the relationship between precipitated Al_3Ti and alloy melt can be expressed as

$$\frac{Al_3Ti_{\mathrm{solid}}}{\text{alloy melt}} = \frac{|BN|}{|BM|} << 1 \quad (8)$$

Most titanium stays in the melt, and the precipitation process can be explained as

$$L \leftrightarrow Al_3Ti + L' \quad (9)$$

With the decrease of melt temperature, the precipitated amount of solid Al_3Ti increases, which can

Table 2 Some properties of phases in composites

Property	Al	Al_3Ti	Mg_2Si
Density/($g\cdot cm^{-3}$)	2.70	3.36	1.99
Elastic modulus/GPa	71	166−230	120
Melting point/K	663	1 340	1085
Heat expansion coefficient (600−700 ℃), α/(10^{-4}℃$^{-1}$)	29.8	11.9	7.5
Hardness (HV)	27	576	450
Lattice constant/nm	$a=b=c$=0.404	$a=b$=0.385, c=0.861,	0.635
Crystal structure	fcc.	DO_{22}(fcc.)	fcc.
Figure of crystal structure	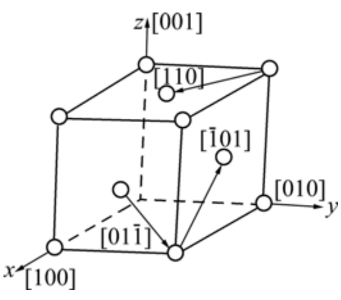	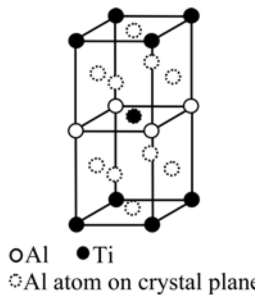	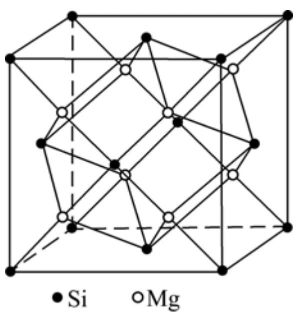

be calculated along the *ANP* curve in Fig.2(b). The process proceeds till to 664 ℃.

At 664 ℃, the peritectic reaction takes place as

$$Al_3Ti+L' \leftrightarrow (Al) \tag{10}$$

The aluminum melt solidifies the surrounding solid Al_3Ti. In the other words, the precipitated Al_3Ti becomes the nucleus of primary aluminum. The whole process can be illustrated by Fig.3.

The behavior of Al_3Ti formation can be disintegrated into two steps. The first is the nucleation. Electromagnetic stirring and high inner energy lead to apparent component fluctuation in melt. So in some certain position the amount of Ti is higher than the average level, which satisfies the nucleus condition of Al_3Ti. The second is the growing up of Al_3Ti nucleus, whether the Al_3Ti phases grow up is subject to the diffusion velocity of Ti element.

3.2 Microstructure of Al_3Ti reinforced phases

In Al_3Ti/6351 composites, Al_3Ti, β-Mg_2Si, Si are all the reinforced phases, among which the volume fraction of Al_3Ti is the highest. Fig.4 shows the morphology of Al_3Ti particles synthesized without and with EMS and fluxes.

In Fig.4(a) the morphology of Al_3Ti exhibits

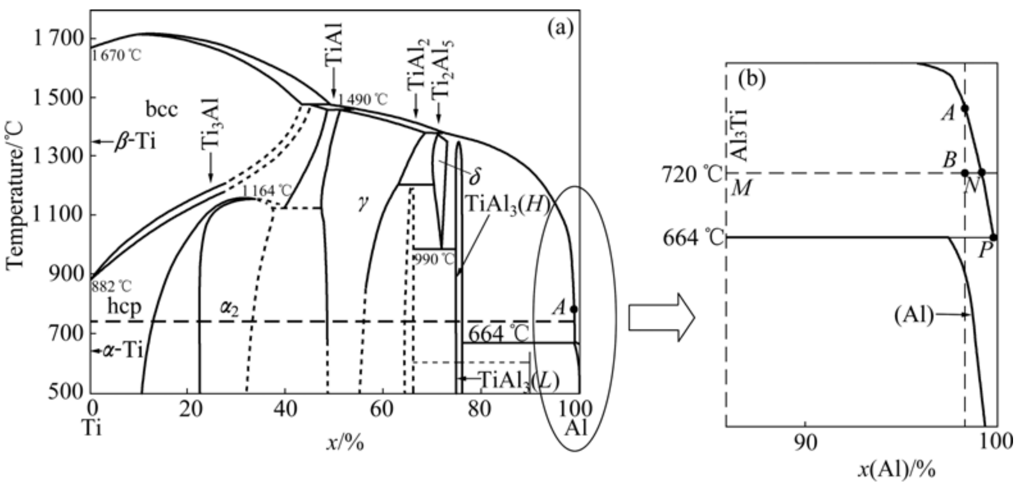

Fig.2 Phase diagram of Al-Ti binary alloy: (a) Al-Ti binary phase; (b) Partial magnification diagram of Fig.2(a)

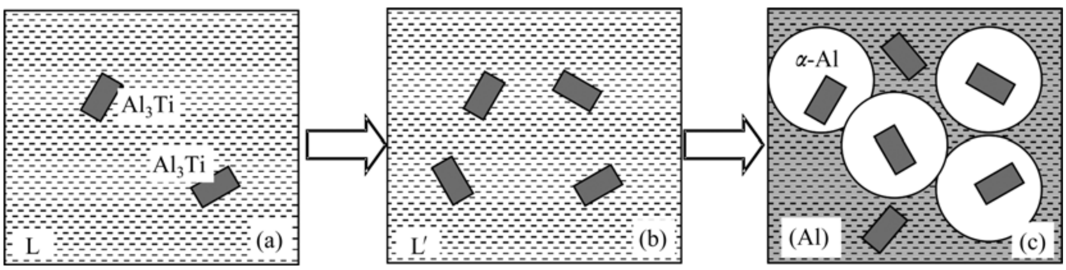

Fig.3 Evolution process of Al_3Ti particles from 720 ℃ to 664 ℃: (a) Melt at 720 ℃; (b) Cooling from 720 ℃ to 664 ℃; (c) Peritectic reaction from 664 ℃

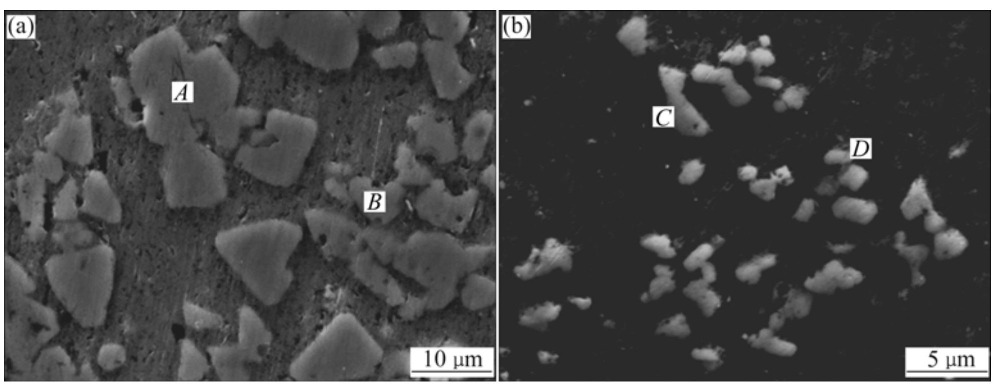

Fig.4 Morphology of Al_3Ti phases in as-cast composites fabricated without (a) and with (b) EMS and fluxes

triangle, quadrilateral and other clumpy shapes, and the sizes of the blocks are in the range of 10−15 μm. In Fig.4(b), the morphology of Al_3Ti does not change obviously, but the sizes of Al_3Ti are refined from 10−15 μm to 2−4 μm. When doped K_2TiF_6 salt with CaF_2 and LiCl, the system temperature decreases from 800 ℃ to 720 ℃. Consequently, the diffusion velocity of Ti element is restricted, which prevents the Al_3Ti from growing[12]. The most important reason is that the electromagnetic stirring force and fluxes addition accelerate the emulsion process of K_2TiF_6. As a matter of fact, the K_2TiF_6 powder enters into the melt via emulsion process. The melting point (T_m) of the mixture K_2TiF_6-15%CaF_2-5%LiCl is 486 ℃, which is much lower than that of K_2TiF_6 salt (the T_m of pure K_2TiF_6 is 682 ℃[13]). At the initial stage of the in situ reaction, the fluxes help the K_2TiF_6 emulsify and react with the molten Al, which enhances the recovery rate of K_2TiF_6 salt. The solid–liquid reaction has been partly changed into a liquid-liquid one. The electromagnetic stirring forces further improve the entering condition of emulsified salt into melt and the dynamics condition of in situ reaction between Al and K_2TiF_6 components. So the nucleation rate of Al_3Ti particles is accelerated and the sizes of particles are refined. The rapid emulsion can be illustrated in Fig.5.

Based on the EDS analysis, it is found that the extra silicon element gathers around the nuclei of Al_3Ti. Fig.6 shows the EDS spectra of some phases in Fig.4.

It can be seen that the components of clumpy phases are different. The components of comparatively bigger ones include Al, Ti and Si elements. From the element ratio listed in Fig.6(a), it is inferred that the phases are Al_3TiSi_x, while the components of comparatively smaller phases consist of Al and Ti elements. From the element ratio listed in Fig.6(b), it is deduced that the phases are Al_3Ti. Considering the relationship between the components and the sizes of clumpy phases, it is presumed that the extra silicon elements in the melt are likely to adhere to the formed Al_3Ti and promote the growth of Al_3Ti.

The reaction between Al_3Ti and Si can be expressed as

$$Al_3Ti+3xSi \rightarrow TiAl_3Si_{3x} \quad (11)$$

Form EDS result the value of x is deduced as 0.073. Eq.(11) can be turned into

$$Al_3Ti+0.22Si \rightarrow TiAl_3Si_{0.22} \quad (12)$$

Fig.7 shows the XRD pattern of Al_3Ti/6351 composites. It demonstrates that the phases in the as-cast composites are α(Al), Al_3Ti and Mg_2Si. The amount of extra silicon is not large enough to be detected.

Fig.8 indicates the TEM morphology of Al_3Ti phase

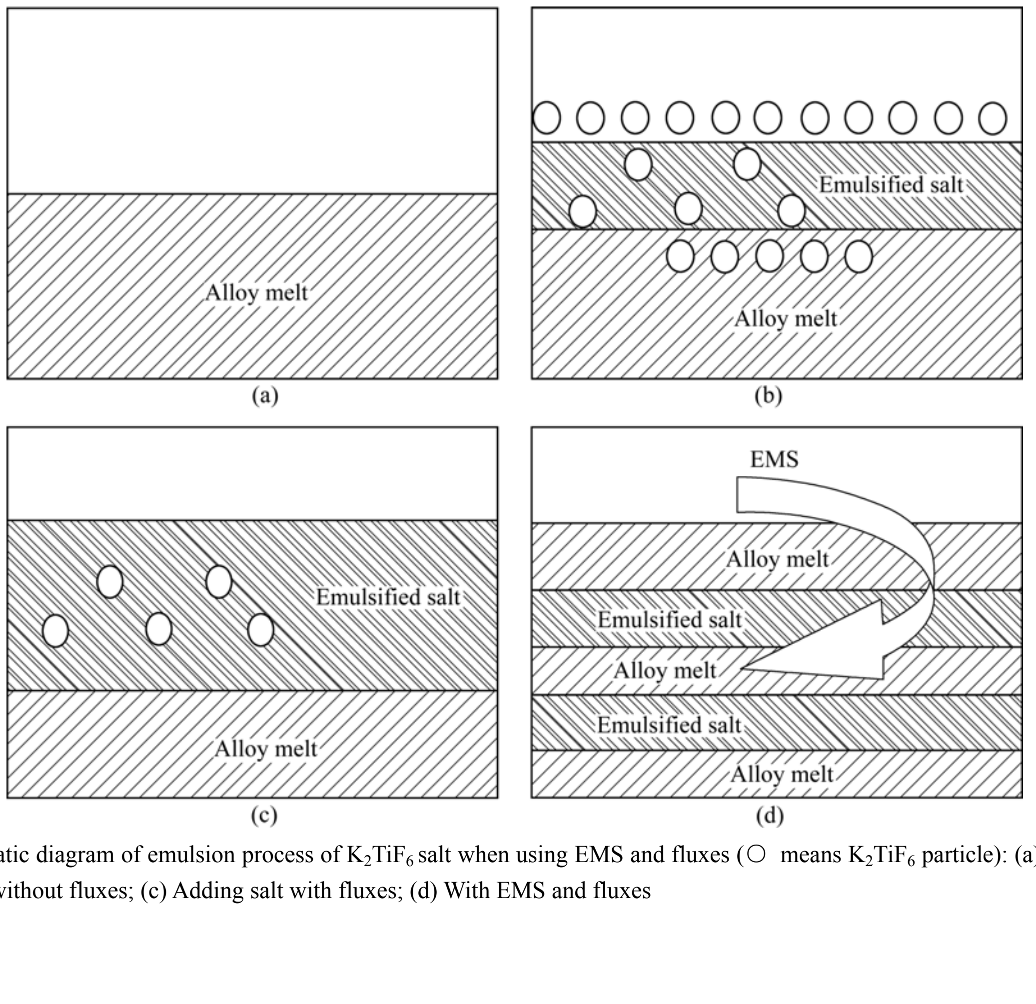

Fig.5 Schematic diagram of emulsion process of K_2TiF_6 salt when using EMS and fluxes (○ means K_2TiF_6 particle): (a) No slat; (b) Adding salt without fluxes; (c) Adding salt with fluxes; (d) With EMS and fluxes

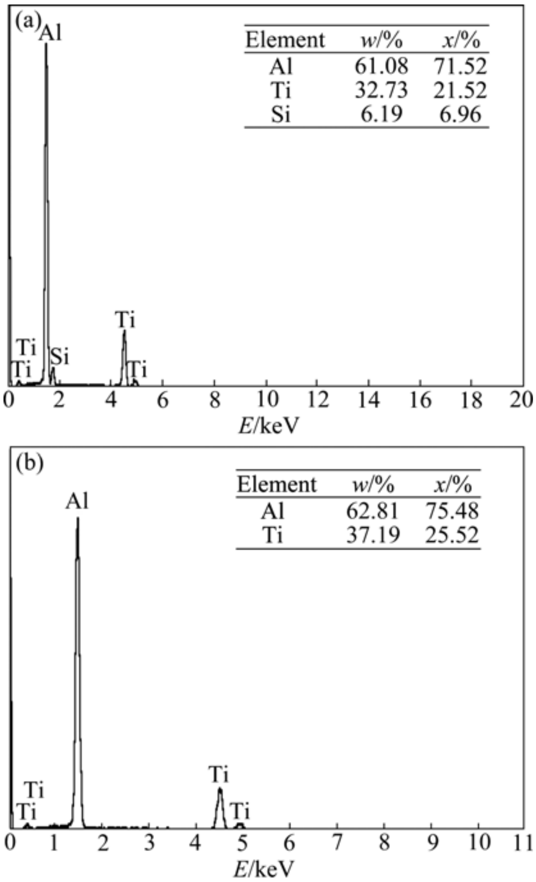

Fig.6 EDS spectra of different phases in Al_3Ti/6351 composites shown in Fig.4: (a) For *A*, *C* areas: AlTiSi eutectic phases; (b) For *B*, *D* areas: AlTi phases

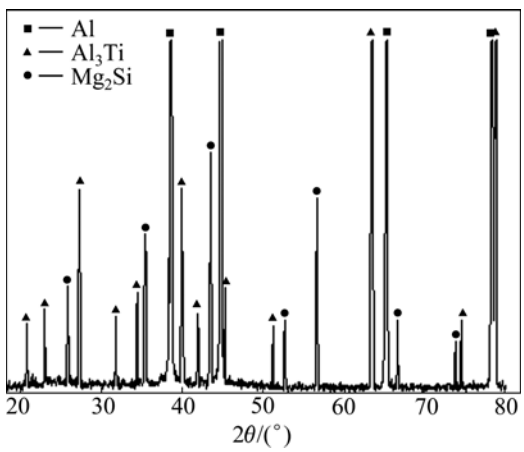

Fig.7 XRD pattern of Al_3Ti/6351 composites

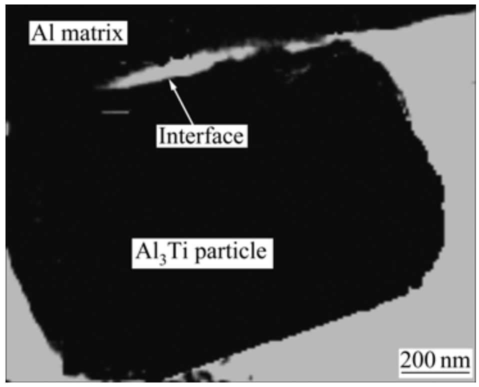

Fig.8 TEM morphology of Al_3Ti phase in as-cast composites

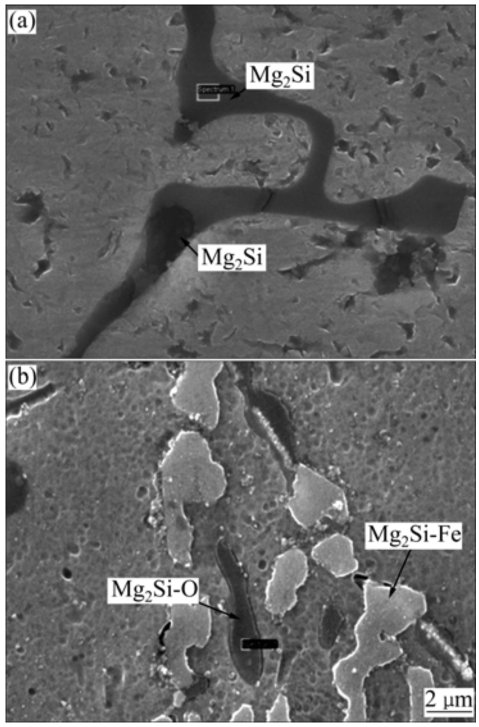

Fig.9 Morphologies of Mg_2Si phases in Al_3Ti/6351composites: (a) Without fluxes; (b) With fluxes

in the as-cast composites. The interface between Al matrix and Al_3Ti particles is clear, where is no unexpected subsidiary product. The bonding state is helpful to increase the mechanical properties of composites.

3.3 Microstructure of Mg_2Si eutectic phases

Fig.9 presents the morphologies of Mg_2Si particles before and after using fluxes. It is shown that without fluxes the Mg_2Si phase exhibits as Chinese character or dendrite[14]. The size of Mg_2Si phase is 8−10 μm. Nevertheless, the patterns of Mg_2Si particles change into polygonal shapes in composites fabricated with fluxes [15]. Meanwhile, the Mg_2Si particles often combine oxygen or ferrum elements together. The average size of Mg_2Si particles is 1−2 μm.

The refinement effects on Mg_2Si can be explained from two views. One is due to the modification effects of K_2TiF_6. The anisotropic growth of Mg_2Si during solidification is suppressed by K_2TiF_6 as modifier[16]. The effect is caused either by poisoning the surface of Mg_2Si nuclei through potassium (K) segregation at the liquid–solid interface or by changing the surface energy of Mg_2Si crystals via lattice distortion due to the insertion of potassium (K) in Mg_2Si lattice[17].

The other reason is due to the formation of Ca_2Si. The Ca atom is released because the CaF_2 reacts with molten Al，which can be illustrated as:

$$CaF_2 = Ca^{2+} + F^- \quad (13)$$

$$2F^- + (2/3)Al = (2/3)AlF_3 + 2e^- \quad (14)$$

$$Ca^{2+} + 2e^- = Ca \quad (15)$$

The Ca_2Si phases generate through the combination reaction between calcium and silicon atoms as:

$$2Ca + Si = Ca_2Si \quad (16)$$

The melting point of Ca_2Si substance which becomes the nuclei of primary Mg_2Si particles is above 900 ℃[18−19]. In the crystal cell of Mg_2Si, the bonding force of Mg-Si is stronger than that of Si-Si, which is beneficial for Mg_2Si particles to precipitate[20].

4 Conclusions

1) The Al_3Ti particles reinforced 6351 aluminum matrix composites were fabricated by K_2TiF_6-CaF_2-LiCl components at 720 ℃ via direct melt reaction method with electromagnetic stirring. The CaF_2 and LiCl acted as fluxes to accelerate the emulsion process of K_2TiF_6 and decrease the in situ reaction temperature from 800 ℃ to 720 ℃.

2) The reinforced phases in the composites are Al_3Ti, $Al_3TiSi_{0.22}$ and Mg_2Si. Compared to composites fabricated without EMS and fluxes, the sizes of endogenetic Al_3Ti or $Al_3TiSi_{0.22}$ particles are refined from 10−15 μm to 2−4 μm. The morphology of Al_3Ti particles exhibits triangle, quadrilateral and other clumpy patterns.

3) The size of Mg_2Si phases is decreased from 8−10 μm to 1−2 μm due to the modification effect of K_2TiF_6 salt and the formation of Ca_2Si.

References

[1] LI Gui-rong, ZHAO Yu-tao, DAI Qi-xun. Fabrication and properties of particles reinforced aluminum matrix composites in-situ synthesized in Al-Zr-O-B system [J]. J Mater Sci, 2007, 42(14): 5442−5447.

[2] TJONG S C. Microstructure and mechanical characteristics of in situ metal matrix composites [J]. Mater Sci Eng A, 2000, 29: 49−113.

[3] UNLUM B S, ATIK E. Tribological properties of journal bearings manufactured from particle reinforced Al composites [J]. Mater Design, 2009, 30(4): 1381−1385.

[4] WANG Hong-ming, LI Gui-rong, ZHAO Yu-tao. Wear behavior of $(Al_3Zr+Al_2O_3)_p$/A359 composites by in situ electromagnetic casting [J]. Rare Metal Mat Eng, 2006, 35(4): 669−672. (in Chinese)

[5] WANG Y, WANG H Y, XIU K. Fabrication of TiB_2 particulate reinforced magnesium matrix composites by two step processing method [J]. Mater Lett, 2006, 60: 1533−1537.

[6] ISIL K. Production of TiC reinforced-aluminum composites with the addition of elemental carbon [J]. Mater Lett, 2005, 59: 3795− 3800.

[7] TJONG S C, WANG G S, MAI Y W. High cycle fatigue response of in situ Al-based composites containing TiB_2 and Al_2O_3 submicron particles [J]. Compos Sci Technol, 2005, 65: 1391−1400.

[8] VARIN R A. Intermetallic-reinforced light-metal matrix in-situ composites [J]. Metall Mater Trans A, 2002, 33(1): 193−197.

[9] LI Gui-rong, ZHAO Yu-tao, WANG Hong-ming, CHEN Gang, DAI Qi-xun, CHENG Xiao-nong. Fabrication and properties of in situ $(Al_3Zr+Al_2O_3)_p$/A356 composites cast by permanent mould and squeeze casting [J]. J Alloys Compd, 2009, 471(1/2): 530−535.

[10] YIN Yu-juan, ZHAO Yu-hou, XIA Yong-xi. Study status of strengthening phase of in-situ aluminum matrix composites [J]. Heat Process Technol, 2006, 35(7): 70−73. (in Chinese)

[11] DURMUŞ H K, OZKAYA E, MERIÇ C. The use of neural networks for the prediction of wear loss and surface roughness of AA 6351 aluminium alloy [J]. Mater Design, 2006, 27(2): 156− 159.

[12] QIN Q D, ZHAO Y G. Nonfaceted growth of intermetallic Mg_2Si in Al melt during rapid solidification [J]. J Alloy Compd, 2008, 462(1/2): L28−L31.

[13] WANG Hong-ming, LI Gui-rong, DAI Qi-xun, LEI Yu-cheng, ZHAO Yu-tao, LI Bo, SHI Guo-min, REN Zhong-ming. Effect of additives on viscosity of LATS refining ladle slag [J]. ISIJ Int, 2006, 46(5): 637−640.

[14] PANIGRAHI S K, JAYAGANTHAN R. Effect of cryorolling on microstructure of Al-Mg-Si alloy [J]. Mater Lett, 2008, 62: 2626−2629.

[15] VARIN R A. Intermetallic-reinforced light-metal matrix in-situ composites [J]. Metall Master Trans A, 2002, 33(1): 193−197.

[16] ZHAO Y G, QIN Q D, ZHAO Y Q. In situ Mg_2Si/Al-Si composites modified by K_2TiF_6 [J]. Mater Lett, 2004, 58: 2191−2194.

[17] HADIAN R, EMAMY M, VARAHRAM N, NEMATI N. The effect of Li on the tensile properties of cast Al-Mg_2Si metal matrix composite [J]. Mater Sci Eng A, 2008, 490(1/2): 250−257.

[18] TANI J, KIDO H. Lattice dynamics of Mg_2Si and Mg_2Ge compounds from first-principles calculations [J]. Comp Mater Sci, 2008, 42: 531−536.

[19] TAKAGI N, SATO Y, MATSUYAMA T, TATSUOKA H, TANAKA M, FENGMIN C, KUWABARA H. Growth and structural properties of Mg_2Si and Ca_2Si bulk crystals [J]. Applied Surface Sci, 2005, 244(1/4): 330−333.

[20] GAO Ying-jun, LI Yun-wen, WANG Tai-cheng, HUANG Chuan-gao, GOU Xian-hua. Keymat analysis of reinforcement effect of Al-Mg-Si alloy [J]. Light Metal, 2005, (2): 55−57. (in Chinese)

(Edited by FANG Jing-hua)